IEEE Access
Multidisciplinary | Rapid Review | Open Access Journal

Received 27 May 2024, accepted 27 June 2024, date of publication 3 July 2024, date of current version 18 July 2024.

*Digital Object Identifier 10.1109/ACCESS.2024.3422675*

RESEARCH ARTICLE

# Development of Adaptive Gripper Enhancing Power Grasp Range and Linearity

**ISSAC RHEE[1], CHUN SOO KIM[1], HEEYEON JEONG[1], SEUNGHWAN UM[1], SEUNG JAE MOON[1], YEONGGWANG SON[1], (Graduate Student Member, IEEE), YONG BUM KIM[2], HO SANG JUNG[2], AND HYOUK RYEOL CHOI[1], (Fellow, IEEE)**

[1]School of Mechanical Engineering, Sungkyunkwan University (SKKU), Suwon, Gyeonggi-do 16419, South Korea
[2]AIDIN ROBOTICS Inc., Anyang, Gyeonggi-do 14055, South Korea

Corresponding author: Hyouk Ryeol Choi (hrchoi@skku.edu)

This work was supported by the Ministry of Trade, Industry and Energy (MOTIE), South Korea, through the Technology Innovation Program, under Grant 20014558.

**ABSTRACT** This paper presents a gripper structure that improves the known potential limitations of curved fingertip movements and the restricted range of objects that can be grasped during power grasp in two-finger adaptive grippers. In the proposed gripper, a Grasshopper mechanism is applied to improve the movement of the fingertips, making it closer to a straight line. Additionally, a grasping method is implemented that allows the fingertips to move towards the palm of the gripper after grasping an object, thereby expanding the size range of objects that can be adaptively grasped. This movement of the fingertips also results in an increase in gripping force. The performance theoretically confirmed through kinematics and force analysis is verified through the development of a prototype. This prototype is used to validate the basic functions of the adaptive gripper and to assess improvements in the fingertip trajectory, demonstrating movement closer to a straight line. Additionally, the improvements in the size range of objects that can be adaptively grasped are verified. The proposed power grasp range ratio shows that the gripper can grasp objects up to 76.7% of the stroke, demonstrating an improved range compared to other two-finger adaptive grippers. Furthermore, the grasping motion of the proposed gripper demonstrates an increase in gripping force in the experiments.

**INDEX TERMS** Mechanical systems, end effectors, robot kinematics.

## I. INTRODUCTION

Research on grippers is primarily focused on adaptive grippers capable of grasping objects of various shapes [1], [2]. In addition to handling various shapes, two-fingered grippers capable of both parallel grasp (precision grasp) and power grasp, as classified in the grasp taxonomy, are commercialized and used in industries [3], [4], [5]. Adaptive grippers with this functionality can achieve either parallel grasp or power grasp depending on the grasp points due to their underactuated structure [6], [7].

However, the movement of the fingertips in adaptive grippers follows a curved trajectory, which becomes larger as the stroke increases. This characteristic results in different gripping positions depending on the object's size. In other words, the gripper's height needs to be adjusted according to the size of the object being grasped. This is especially important when using the gripper with various objects, as being aware of the target object's size is vital for executing the desired grasping action. Additionally, due to the nature of the arc movement, even when attempting to grasp an object with a parallel grasp, the movement of the fingertips along the arc trajectory can result in the object being grasped in the adaptive grasp area. This can cause the gripper to perform a power grasp unintentionally. Moreover, unlike parallel grasp, power grasp has limitations on the size of objects that can be grasped, which can lead to grasp failures [4], [8]. For example, the Robotiq gripper, with a stroke of 140mm, can grip objects with a minimum diameter of 90mm in power grasping. In other words, when an object is gripped within the power grasping area, it is difficult to grip objects with a diameter of less than 90mm [4].

The associate editor coordinating the review of this manuscript and approving it for publication was Tao Liu.

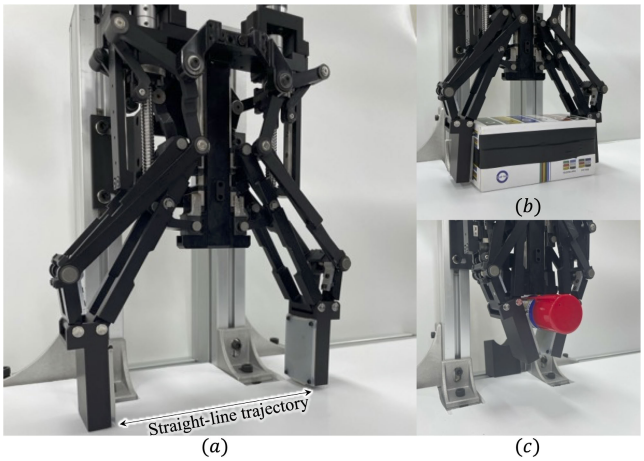


**FIGURE 1.** Features of the proposed gripper. (a) The proposed gripper enabling the fingertip to perform a motion close to a straight line. (b) Capability to grasp objects of various sizes at the same height based on the Grasshopper mechanism. (c) Palmar power grasp moving towards the palm after grasping.

Therefore, in this paper, the gripper shown in Fig. 1 is proposed to address the aforementioned issues. The proposed gripper is designed to enable both parallel grasp and power grasp, with the trajectory of the fingertips approximating a straight line. Additionally, the gripper implements the palmar pinch and palmar power grasp functions, allowing the fingertips to move towards the palm direction. This design reduces the minimum size of objects that can be grasped relative to the stroke, thereby increasing the range of object sizes that can be adaptively grasped. Furthermore, this structural characteristic includes a mechanism that increases the gripping force.

The remainder of the paper is organized as follows: Section II introduces the related work concerning the functionality of the proposed gripper. Section III presents the problem formulation. In Section IV, a detailed explanation of the mechanisms applied to the proposed gripper, categorized by their intended functions, is provided. Section V presents the kinematics and force analysis of the proposed gripper mechanism. Section VI describes the design of the gripper and its performance. The experiment for the verification of the gripper is presented in Section VII. Finally, in Section VIII, the conclusion of our research and future work are presented.

## II. RELATED WORK

Several studies on two-finger adaptive grippers, as shown in Table 1, proposed methods to implement the fingertip movement, which usually follows an arc trajectory, as a straight line. First, there is a method that achieves linear fingertip movement by using a parallel gripper base and applying adaptive links to the fingers. D.Yoon et al proposed a link structure that attaches fingers to a parallel gripper base, implementing human-like finger motions in an adaptive gripper design [9]. This allows for safe object grasping even when in contact with the environment. M. Aqib et al.

**TABLE 1.** Two-finger adaptive gripper with linear trajectory.

| Name | Applied method |
|---|---|
| Fully passive robotics finger [9] | Parallel gripper base |
| Multi-functional adaptive gripper [10] | |
| Two-way self adaptive gripper [11] | |
| Self-adaptive robot hand [13] | Rack and pinion |
| Self-adaptive robot hand [14] | Gear train, slider mechanism |
| Self-adaptive underactuated hand [15] | Sliding base mechanism |
| Hoecken gripper [16] | Hoeckin linkage mechanism |

also implemented a mechanism based on the operation of a parallel gripper, incorporating a link structure for the finger part and proposing a design that enables scooping as well [10]. A parallel gripper base was similarly used in [11], and adaptive grasping was implemented with a relatively simple structure, incorporating springs, unlike the previously proposed gripper.

However, these grippers have a limitation in that they cannot have a stroke larger than the base of the parallel gripper, as they utilize the parallel gripper base. Consequently, their stroke is relatively smaller compared to adaptive gripper structures composed of link mechanisms [12].

There are studies focused on implementing a straight fingertip trajectory based on the typical adaptive gripper structure, where the links rotate causing the fingertips to move in a curved path. Li and Zhang implemented a straight fingertip trajectory using a rack and pinion mechanism along with a slider and link structure [13]. Similarly, a gripper was also proposed to prevent the arc movement of the fingertip trajectory using a gear train and slider mechanism [14]. Li et al. proposed a method where a sliding base mechanism is applied to the basic finger link structure. This design allows the base with the actuator to move while the finger performs the grasping motion, resulting in a straight fingertip trajectory [15]. Liu and Zhang developed the Hoecken gripper, which implements a Hoekin linkage mechanism using linkages, rollers, and a slot configuration to achieve a straight fingertip trajectory [16]. The proposed structures have implemented a straight fingertip trajectory using link configurations or a combination of gears and slides. However, there are still limitations regarding the range of objects that can be grasped during adaptive grasping, and a finger mechanism to address this issue has not yet been proposed.

## III. PROBLEM FORMULATION

In this paper, specific limitations identified in existing two-finger adaptive grippers are aimed to be overcome. These limitations include:

1) The requirement for varying grasping heights according to the size of the object due to the curved motion of the fingertips in conventional adaptive grippers. This characteristic becomes more pronounced as the stroke of the gripper increases.
2) The constraints on the size of objects that can be grasped during a power grasp.

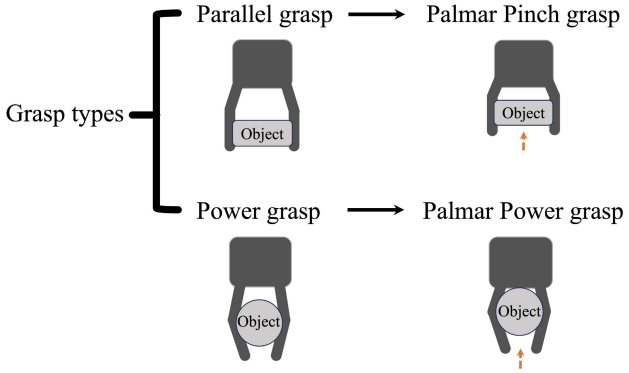


**FIGURE 2.** Grasp types of the proposed gripper. The transition from a parallel grasp and power grasp to a palmar grasp (including a palmar pinch grasp and palmar power grasp) constitutes a continuous sequential motion.

To address these issues, a gripper designed to achieve nearly linear fingertip trajectories is proposed, enhancing the consistency of gripping heights across different object sizes. Furthermore, our design incorporates a mechanism that allows the fingertips to move towards the palm direction during a power grasp. This adjustment significantly expands the range of objects that can be securely gripped. Additionally, this mechanism facilitates an increase in gripping force without requiring additional motor torque. The model and functions of the proposed gripper are illustrated in Fig.1. By employing a mechanism different from that described in previous literature, this design achieves a trajectory of the adaptive gripper fingertips that is more linear, thus compensating for the grasping failures due to the curved trajectory of fingertips in traditional adaptive grippers. In addition, a mechanism has been added to enable a palmar power and palmar pinch grasp mode, which are not available in existing commercial adaptive grippers.

The classification of the grasping methods of the proposed gripper, including the aforementioned palmar pinch grasp and palmar power grasp, is depicted in Fig.2. Unlike the pinch grasp of adaptive grippers, where the fingertip follows a curved trajectory, the proposed gripper's fingertip moves along an approximate straight trajectory, thus defined as a parallel grasp. Following this, the movement towards the palm direction is defined as a palmar pinch grasp. For the power grasp, as it grasps in a manner similar to adaptive grippers, it is defined under the same name, and the subsequent movement towards the palm is defined as a palmar power grasp.

Specifically, the palmar pinch grasp is inspired by one of the human hand's grasping methods and offers the advantage of exerting greater force on the object compared to the tip pinch method [17]. As for the palmar power grasp, a novel motion has been defined in the direction of the gripper's palm, thanks to the proposed mechanism. This mode allows for improvement in the limitation on the minimum object size for power gripping while still providing a large stroke. Furthermore, this mechanism also increases the gripping force.

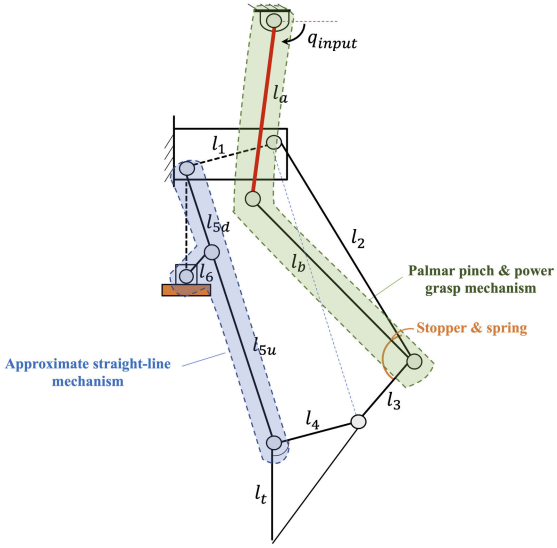


**FIGURE 3.** Linkage configuration of the proposed gripper: mechanisms for linearizing curved trajectories and enabling palm movement to improve the limitation of object size in the power grasp.

## IV. PRINCIPLES OF GRIPPER MECHANISM

The proposed gripper, configured based on a 5-bar linkage which is a standard configuration for adaptive grippers, incorporates two mechanisms as depicted in Fig. 3 to introduce novel functionalities. These enhancements include the implementation of an approximately straight trajectory at the fingertip and the execution of both Palmar pinch grasp and Palmar power grasp. The principles behind the mechanisms for each proposed functionality are explained in detail.

### A. FINGERTIP TRAJECTORY - APPROXIMATE STRAIGHT LINE

A number of approaches exist to solve the above arc trajectory problem as mentioned in the previous section [13], [14], [15], [16]. In order to solve the problem with a simpler mechanism configuration, the author considered a strategy that could approach an approximate straight line.

In the 5-bar linkage used in the existing adaptive gripper, the Grasshopper mechanism is applied to change the curved path into a straight line [18]. Although numerous mechanisms exist that can implement a straight-line motion, the proposed linear mechanism was applied due to its advantage of enabling a large stroke in comparison to the short crank length [19]. The grasshopper mechanism is a method that can draw a straight line or a trajectory close to a straight line in partial sections due to the ratio of the three link lengths as shown in Fig. 4 below [18], [19]. For instance, if the lengths of the three links are the same, a perfectly straight line can be realized. In our case, considering the space of the gripper mechanism, the error of the approximate straight line is carried out by aiming for 1mm inside.

In order to approximate a straight line in relation to the mechanism, the following formula was constructed. First, the value of $sin(\theta_1)$ for the length $l_{5d}$ is the same as $sin(\varphi)$

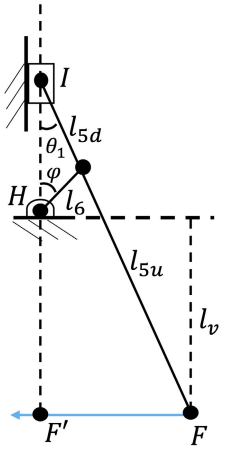


**FIGURE 4.** Grasshopper mechanism.

for length z. After constructing the expression, it can be re-expressed as follows.

$$\sin\theta_1 = \frac{l_6}{l_{5d}}\sin\varphi \tag{1}$$

$$\cos\theta_1 = \sqrt{1-\sin^2\theta_1} = \sqrt{1-(\frac{l_6}{l_{5d}}\sin\varphi)^2} \tag{2}$$

To draw a straight line with an angle $\varphi$ within a certain range, the length $l_v$ must be kept constant. Therefore, the following formula is formed.

$$l_v = l_{5u}\sqrt{1-(\frac{l_6}{l_{5d}}\sin\varphi)^2} - l_6\cos\varphi = constant. \tag{3}$$

The equation for the minimizing error of straight-line is as

$$\min_{l_{5d},l_{5u},l_6}[L_{desired} - l_v]^2 \tag{4}$$

where $L_{desired}$ is set as a reference value of $l_v$ according to the required gripping area of the gripper. Alternatively, the initial value of $l_v$ may be set according to the link length at the position of the initial gripper state.

### B. ENHANCING POWER GRASP CAPABILITY AND GRASPING FORCE

In the case of a general adaptive gripper, as the length of the stroke increases, the size of the object that can be gripped in the power grasp area becomes larger. Therefore, to solve this problem, A base transition mechanism was applied so that when the object is grabbed by the gripper, it can be gripped in the direction of the gripper's palm. Additionally, by applying this mechanism, even with the same torque, the fingertip force applied to the object increases as it moves in the palm direction.

The mechanism related to enhancing power grasp capability and grasping force is shown in Fig. 5. The principle of the mechanism is illustrated in three steps in Fig. 5. To facilitate the previously discussed functionality, the force must always be directed towards the palm throughout all stroke ranges in the underactuated finger configuration, which integrates the

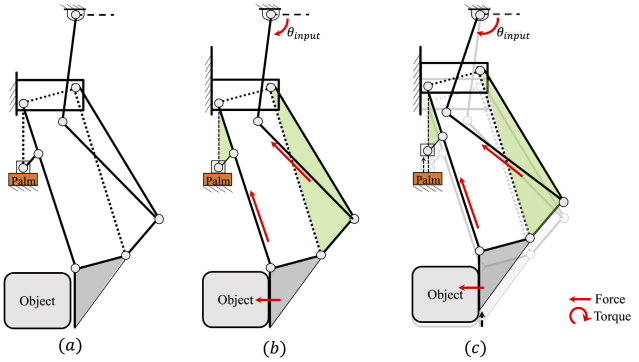


**FIGURE 5.** Palmar pinch & power grasp mechanism. (a) Parallel motion unless contact with the object. (b) Contact with the object (c) Fingertip transition to the palm(Palmar pinch & power grasping motion depending on the equilibrium point of the fingertip).

links of the Grasshopper mechanism within a 5-bar linkage configuration. Consequently, a dual-linkage approach was employed to actuate the movement of the gripper. As the proposed gripper is designed for bin picking, the fingertip is assumed to point toward the ground, which is the direction of gravity. If the gripper structure is to be applied in various environments beyond bin picking, an extension spring or a constant load spring can be attached to the part of the gripper where the palm falls to provide tension support.

The first schematic (a) shows the initial state of the gripper. If there is no object thereafter, the fingertip trajectory of the gripper moves in an approximately straight line through the Grasshopper mechanism. When an object, assumed to be stationary and placed on the ground, comes into contact with the gripper, the green triangle is fixed as a single rigid body as shown in (b) of Fig. 5, and the torque generated by the actuator rises upward due to the direction of the force at the front link. This is expressed in (c) of Fig. 5. Due to the characteristic of this mechanism, the object moves in the palm direction during power grip, enabling power grip on objects that are relatively smaller than general adaptive grippers. In this case, the gripping range of a small object is dependent on the possible length of the base transition. This is explained in the next section.

Another effect of the proposed base transition mechanism is that the moment arm becomes shorter as the distance between the actuator and the fingertip decreases during base transition so that the force increases at the same torque. The analysis of the rate of increase in fingertip force according to the base transition is also covered in the next section.

## V. KINEMATICS & FORCE ANALYSIS

The illustration of the schematic of the proposed gripper is shown in Fig. 6. The figure encompasses a comprehensive schematic diagram as presented in (a), components relevant to the Grasshopper mechanism as highlighted in (b), and a comprehensive description of the relationship between the input angle $q_a$ and $q_2$ as depicted in (c).

The structure is composed of 10 links, 9 revolute joints, and 3 prismatic joints, featuring 3 degrees of freedom. Link $l_{5u}$

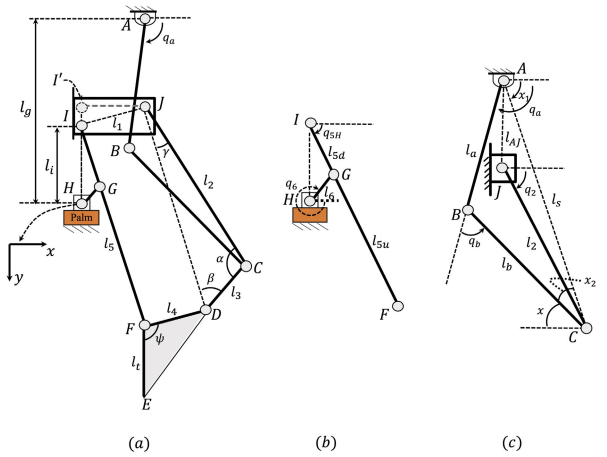


**FIGURE 6.** Schematic of the proposed gripper. (a) Overall linkage configuration. (b) Grasshopper mechanism part. (c) Relationship between $q_a$, $q_b$, and $q_2$ of link 2 ($l_2$) associated with input link ($l_a$).

serves as the proximal phalanx and $l_t$ as the distal phalanx. Joint A is where the torque from the actuator is applied, initiating movement in the clockwise (CW) direction from its initial position. Additionally, the stopper and torsion spring located at joint C maintain the parallel motion of the object before it is grasped and preserve its posture.

It is necessary to derive the equations for kinematics and forces to verify if the motion expected according to the configuration of each link of the proposed gripper is implemented. This includes explaining the kinematics equations and determining the minimum size of objects that can be grasped during a Palmar power grasp based on the finger link structure. Additionally, the relationship between the forces acting on each joint of the gripper when the object is grasped based on the input torque is described in detail.

### A. KINEMATIC ANALYSIS

The relationship between the position of the Fingertip and the movement of $q_a$ was determined using the geometrical relationship in each part of Fig. 6. The proposed gripper consists of parallel grasp motion, power grasp motion, and power grasping motion, and the fingertip position changes according to each constraint, so it is necessary to derive the relationship equation for each scenario.

In the case of parallel motion, for the convenience of calculation, $q_a$ is first obtained based on $q_6$, and the equation is constructed to obtain the trajectory during parallel motion. Considering that the values of $\alpha$, $\beta$, and $\gamma$ are fixed by the stopper and spring, the square JDFI is composed of a parallelogram mechanism, so the angle of link FD is maintained while moving. This relationship is established in Fig. 6 (b), where $q_{5H}$ satisfies the following equation.

$$q_{5H} = \gamma + q_2 \tag{5}$$

Furthermore, the length of $l_i$ can be expressed as follows through $q_2$ and $q_6$.

$$l_i = |l_6 \sin q_6| + l_{5d} \sin(\gamma + q_2) \tag{6}$$

The interconnection between $q_6$ and $q_2$ is depicted through the equation of the links that constitute the Grasshopper mechanism in Fig. 6 (b). The equation is as follows:

$$q_2 = \cos^{-1}\left[\frac{l_6 \cos q_6}{l_{5d}}\right] - \gamma \tag{7}$$

Utilizing this equation allows for the determination of the length value $l_i$. Since $l_g$ is maintained constant during parallel motion, it consequently enables us to derive the value of length $l_{AJ}$.

The length of $l_s$ in Fig. 6 is as

$$l_s = \sqrt{(l_2 \cos q_2)^2 + (l_2 \sin q_2 + l_{AJ})^2} \tag{8}$$

The values of $x_1$, $x_2$ and $x$ is obtained as follows.

$$x_1 = \cos^{-1}\left[\frac{l_2 \cos q_2}{l_s}\right] \tag{9}$$

$$x_2 = \cos^{-1}\left[\frac{l_b^2 + l_s^2 - l_a^2}{2 l_b l_s}\right] \tag{10}$$

$$x = x_1 - x_2 \tag{11}$$

Therefore, $q_a$ and $q_b$ are obtained using the above equation.

$$q_a = \cos^{-1}\left[\frac{l_2 \cos q_2 - l_b \cos x}{l_a}\right] \tag{12}$$

$$q_b = q_a - x - \pi \tag{13}$$

In the case of power grasping action, the object is firmly grasped within the internal region of the gripper composed of two phalanges ($l_5$ and $l_t$), with link 5 and $l_{AJ}$ being fixed. This results in the square JDFI being viewed as a four-bar mechanism. Therefore, by utilizing geometric relationships, it is possible to derive the relationship between $q_t$ and $q_a$ as $q_a$ changes. For the palmar power grasping motion, it is observed that the motion of links A and B causes the remaining links to move downwards, leading to a sliding motion of joint C. Consequently, by analyzing the positional change of link C in response to variations in $q_a$, one can establish the relationship between the position of link C and changes in $q_a$.

### B. MINIMUM OBJECT SIZE FOR PALMAR POWER GRASPING

The palmar power grasp motion generates specific characteristics that decrease the minimum size of objects that can be grasped during power grasp. To determine the actual size of objects that can be grasped, a schematic shown in Fig. 7 was constructed. In particular, Fig. 7 (a) presents the conditions necessary for determining the minimum object size that can be grasped during palmar power grasp, while Fig. 7 (b) shows the variables required to calculate the minimum object size. Although objects can take various shapes, for our study, the minimum object size was calculated by considering the shape of a circle, which is a two-dimensional representation of a cylinder. This allowed us to determine the minimum size of objects that can be grasped during palmar power grasp motion.

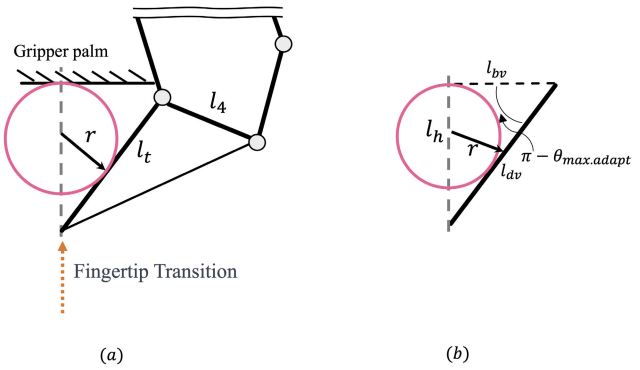


**FIGURE 7.** Schematic for determining the minimum size of the object in palmar power grasping.

For condition (a) of calculating the minimum object size, The two fingers are considered to be in contact with a vertical line at the center of the palm in the gripper, moving at the maximum adaptive angle. In condition (b), the grasped cylindrical object is simplified by assuming that it is in contact with the two fingers. As previously mentioned, this simplification can be represented as an inscribed circle in a triangle in the two-dimensional plane. In Figure 7, the variables $l_h$, $l_{dv}$, and $l_{bv}$ are sequentially represented as follows.

$$l_h = l_t \sin(\pi - q_{max.ad}) + l_{5u} \sin q_{5H} - l_6 \sin q_6 - l_{max.trans} \tag{14}$$

where $q_{max.ad}$ is the maximum adaptive angle and $l_{max.trans}$ is maximum length of the fingertip transition. The $l_{dv}$ and $l_{bv}$ are derived as follows.

$$l_{dv} = \frac{l_h}{\sin(\pi - q_{max.ad})} \tag{15}$$

$$l_{bv} = \sqrt{l_{dv}^2 - l_h^2} \tag{16}$$

Since the given circle can be considered as the inscribed circle of the triangle, it is possible to determine the radius of the inscribed circle using the geometric properties of the triangle and the area expressed in terms of the inscribed circle's radius.

$$r = \frac{l_{bv} l_h}{l_{dv} + l_{bv}} \tag{17}$$

### C. FORCE ANALYSIS

In order to analyze the relationship between the forces applied by the fingertip on the object and the change in force in the palm direction during power grip, a quasi-static modeling approach is used [20], [21], [22].

The virtual work is expressed as follows.

$$\mathbf{t}^T \boldsymbol{\omega_i} = \mathbf{f}^T \mathbf{v} \tag{18}$$

where $\mathbf{t}$ is composed of the torque transmitted by the actuator and the torque due to the torsion spring. $\boldsymbol{\omega_i}$, therefore, represents the angular velocity of link a and the angular velocity of $\alpha$. $\mathbf{f}$ and $\mathbf{v}$ represent the force and the velocity generated by the fingertip. Consequently, the relationship between the input torque and the resulting force acting perpendicular to the finger joint is obtained as follows:

$$\mathbf{f} = \mathbf{J_g}^{-T} \mathbf{J_c}^{-T} \mathbf{t}. \tag{19}$$

The equation related to the forces generated as the finger moves towards the palm after grasping an object in palmar power grasping mode is derived as follows:

$$\mathbf{f_p} = \mathbf{J_p}^{-T} \mathbf{t}. \tag{20}$$

The detailed derivations of the related equations can be found in the appendix A.

## VI. GRIPPER DESIGN & PERFORMANCE

The gripper developed based on the proposed mechanism is described, and theoretical values are analyzed to determine the extent to which the fingertip trajectory can approximate a straight-line movement. Additionally, it is verified whether the proposed gripper can grasp smaller objects than conventional adaptive grippers during a palmar power grasp and whether there is an increase in grasping force based on the equations described in the previous section.

### A. GRIPPER DESIGN & IMPLEMENTATION

In order to verify the functionality of the proposed mechanism, a prototype is fabricated. The stroke of the gripper is set to 150mm. The sequence of selecting link lengths is as follows. Firstly, the link lengths for the Grasshopper mechanism are determined, and then the link lengths for the 5-bar linkage are obtained. The link lengths for palmar pinch & palmar power grasp, $l_a$ and $l_b$, are selected based on the requirement that the fingers move by 40mm in the palm direction. Additionally, the angle between link $l_a$ and $l_b$ is set to ensure that the rate of movement towards the base direction, where force transmission is more efficient, does not significantly vary with the rotational movement of link $l_a$ during the return to the original position after palmar pinch & palmar power grasp motion.

Fig. 8 (a) and (b) show the proposed gripper model. (a) presents the size and stroke information of the gripper, while panel (b) illustrates the components used for each function in the assembled gripper. It separates the structure that can implement the functions of making the trajectory of the fingertip similar to a straight line, adaptive gripper function, and increasing the grasping force.

The gripper's operation involves the actuator transmitting force to the link through the ball screw, which then transmits torque to the main link structure composed of the Grasshopper mechanism, 5-bar linkage, and power grasp linkage via link a. Fig. 8 (c) presents the fabricated prototype of the proposed gripper. An 80-Watt motor (ECX22, MAXON) is used for each finger, and the total weight of the gripper is 1.3 kg. The detailed specification of the proposed gripper is shown in Table 2.

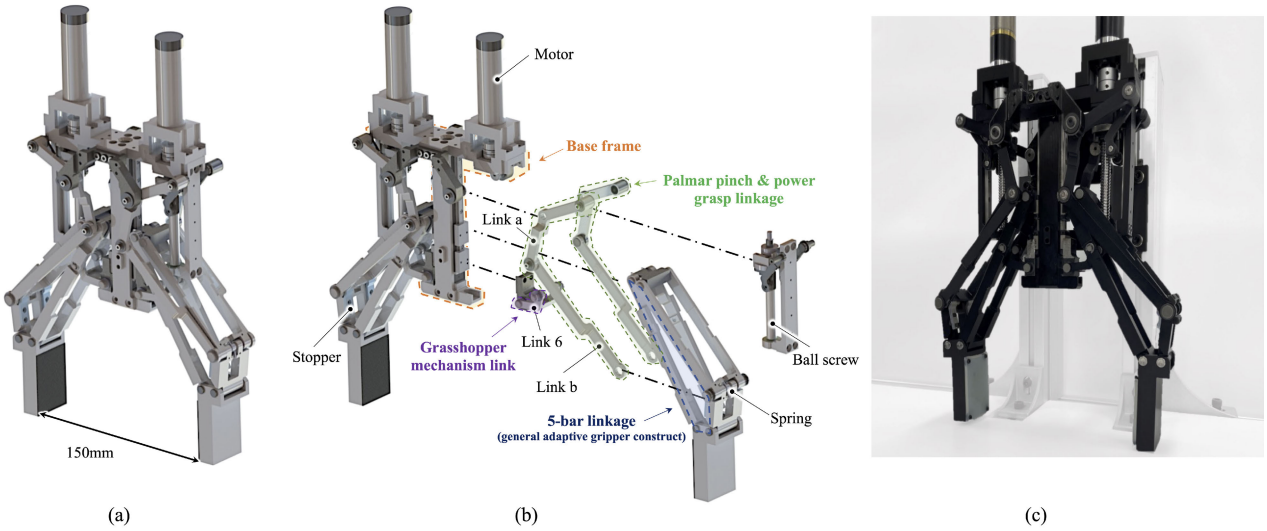


**FIGURE 8.** (a) Gripper modeling. (b) Gripper detail configuration, depicting the main function of the proposed gripper, comprised of an adaptive link structure with a 5-bar linkage, a Grasshopper mechanism link that implements an approximately straight trajectory, and link components that facilitate palmar pinch and palmar power grasps. (c) Fabricated prototype gripper.

**TABLE 2.** Specification of prototype gripper.

| | |
|---|---|
| Size | 201 × 335 × 55 (W × H × T) |
| Weight | 1.3kg |
| Stroke | 150mm |
| Minimum object diameter | 35mm |
| Maximum fingertip force | 140N |
| Motor continuous torque | 128.1mNm |

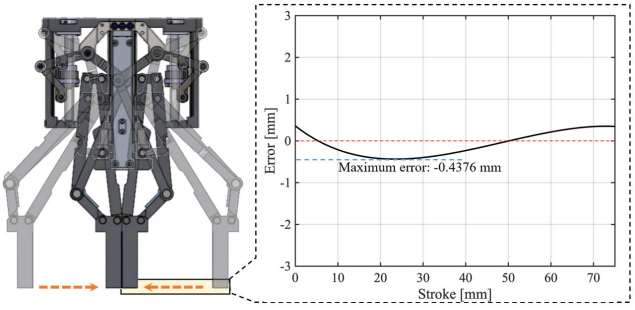


**FIGURE 9.** Comparison of deviation between fingertip trajectory and desired linear path.

### B. FINGERTIP TRAJECTORY

In Fig. 9, the y-axis denotes the discrepancy between the average height change during finger closure and the actual height change during motion. The maximum deviation from the reference height is 0.4376mm, and the root means square error (RMSE) is 0.288mm. As the gripper's height difference is less than 0.5mm, and the deviation from a straight line compared to the stroke is $2.9 \times 10^{-3}$, it can be regarded as following a trajectory close to linear.

### C. MINIMUM SIZE OF THE OBJECT IN PALAMR POWER GRASP

The proposed gripper is equipped with a power grip function that allows the fingers to move towards the palm direction upon grasping an object, enabling it to handle smaller objects in the power grasp area than other adaptive grippers. Based on the link length of the manufactured gripper, theoretical calculations confirm its ability to grasp cylinders with a minimum diameter of 35mm.

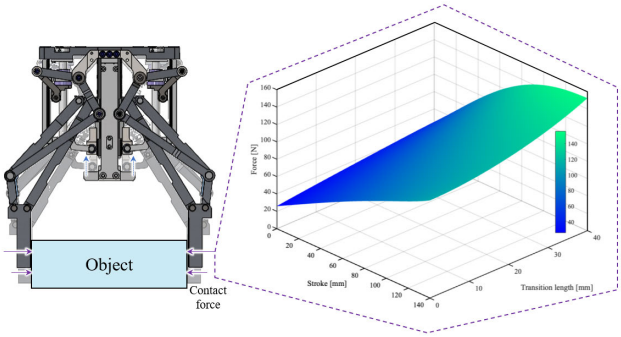


**FIGURE 10.** Variation of fingertip force in relation to the transition length moving in the palm direction due to palmar pinch grasp in each stroke.

The proposed gripper has an additional characteristic resulting from the power grasp, namely an increase in contact force on the object as the fingertips move toward the palm. Despite a fixed input torque location, the force acting on the object increases as the fingertips move towards the palm, reducing the distance between the point of force application and the input torque location.

### D. VARIATION IN FINGERTIP FORCE WITH PALMAR PINCH GRASP

To obtain theoretical values, the fixed length $l_g$ in parallel motion is gradually reduced by 1mm increments up to a maximum possible distance of 40mm to the palm. Using (19), the variation in the force applied to the fingertip within the stroke range can be derived, as illustrated in Fig. 10.

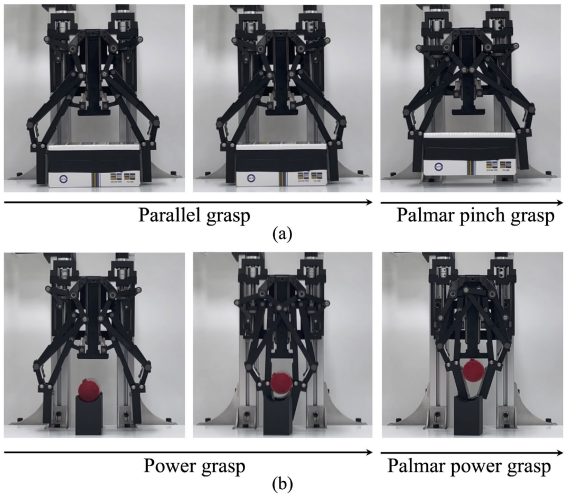


**FIGURE 11.** Basic motion of the proposed gripper: (a) Parallel grasp with palmar pinch grasping (b) power grasp with palmar power grasping.

## VII. EXPERIMENT

The performance of the proposed gripper was validated through three experiments. Initially, basic motions were tested to verify whether the fingertips move in an approximately straight trajectory and whether the Palmar pinch & Palmar power grasp movements were implemented. The ability of the proposed gripper to grasp objects of various sizes was tested, and its performance was compared to the theoretically calculated grasping sizes during Palmar power grasp.

Subsequently, comparisons with the 2F-140 from ROBOTIQ, one of the state-of-the-art two-finger adaptive grippers, were made to examine the general trajectory of adaptive gripper fingertips and to assess differences in the size limitations of objects that can be grasped during power grasp between the conventional power grasp and the proposed gripper's Palmar power grasp. Additionally, a comparison table was provided to illustrate the grasping range during power grasp based on performance data from other two-finger adaptive grippers.

Lastly, the increase in the gripping force of the proposed gripper during Palmar pinch grasp and Palmar power grasp, where the fingertips move towards the palm, was experimentally verified using a force measurement sensor to ensure that the theoretically confirmed increase in gripping force was realized in practice. During the experiments, the gripper was controlled utilizing a controller configured through the TCP-based Robot Operating System (ROS1), with the motor driver and gripper controller employing EtherCAT communication for their setup.

### A. GRIPPER MOTION & LINEARITY IMPROVEMENT

Fig. 11 illustrates how the gripping motions, previously classified as types of grasp, are executed when grasping objects. Initially, it is observed that a parallel grasp is achieved with a box object, followed by a continuous motion into a palmar pinch grasp, as shown in Fig. 11 (a). In Fig. 11 (b), it is evident that when grasping occurs in the power grasp area, the motion continuously transitions into a palmar power grasp following the initial power grasp.

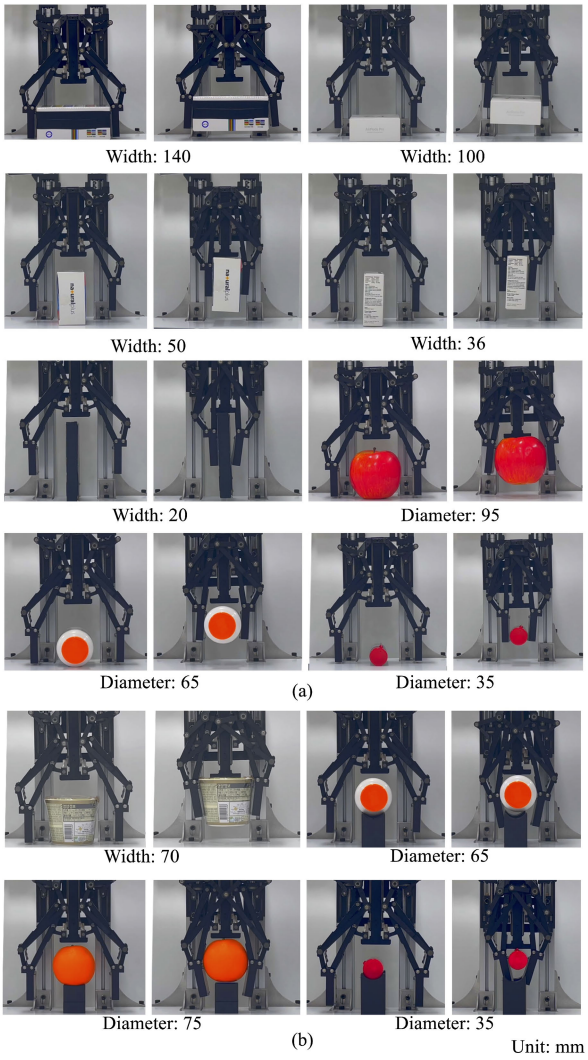


**FIGURE 12.** (a) Gripper verification for capability of various sizes in the parallel and palmar pinch grasp (b) Gripper verification for capability of various sizes in the power and palmar power grasp.

### B. PERFORMANCE OF PALMAR PINCH GRASP & PALMAR POWER GRASP

Validation of these grasping methods was performed by grasping various objects, as illustrated in Fig. 12. The results of grasping various objects using parallel and palmar pinch grasps of different sizes are presented in Fig. 12 (a). The experiment utilized box-shaped objects with sizes of 20mm, 36mm, 50mm, 100mm, and 140mm, cylinder-shaped objects with sizes of 35mm, and 65mm, and spherical-shaped objects with a diameter of 95mm. The figures show that the objects are first grasped with a parallel grasp while on the ground, followed by a palmar pinch grasp to move the object in the direction of the gripper palm.

**TABLE 3. Comparison with state-of-the-art and developed adaptive grippers.**

| Adaptive gripper with two fingers | Stroke | Minimum object diameter (for power grasping) | Power grasp range ratio | Fingertip trajectory |
|---|---|---|---|---|
| 2F-140 [4] | 140mm | 90mm | 35.7% | Arc |
| AG-105-145 [7] | 145mm | Unknown | Unknown | Arc |
| Two-Way Self-Adaptive gripper [11] | 90mm | 0mm | 100% | Straight line |
| Hoekin gripper [16] | 140mm | 60mm | 57.1% | Straight line |
| Proposed gripper | 150mm | 35mm | 76.7% | Straight line |

In Fig. 12 (b), the experimental results of grasping objects with power grasp and palmar power grasps are presented. The target objects included cylinder-shaped objects with diameters ranging from 35mm to 65mm, a spherical-shaped object with a diameter of 75mm, and a symmetrical cup shape. The figures show that the objects are grasped adaptively, and the palmar power grasp function is used to perform continuous movements. It was confirmed that palmar power grasping was possible for objects with a calculated diameter of up to 35mm.

To quantify the performance, the range of objects that can be grasped during a power grasp is defined as the power grasp range ratio. The power grasp range ratio, defined as the ratio of the size of objects that can be grasped during a power grasp relative to the stroke, is a measure used to evaluate the gripper's performance and is expressed as a percentage (%). This signifies that the proposed gripper is capable of grasping objects approximately 76.7% the size of an object with a diameter based on a 150mm stroke. These results demonstrate the capability of the gripper to adapt to different object shapes and sizes.

### C. COMPARISON WITH STATE-OF-THE-ART ADAPTIVE GRIPPERS

A comparison table of the power grasp range ratio for state-of-the-art and developed two-finger adaptive grippers is presented in Table 3. As shown in Table 3, the power grasp range ratio includes a value of 100%, which is achievable because power grasp and parallel grasp share the same area when using a parallel gripper-based design. However, as previously mentioned, this design has the limitation of a relatively small stroke due to the parallel gripper base [12]. The proposed gripper, on the other hand, utilizes a basic adaptive link structure, demonstrating a wide stroke and a high power grasp range ratio of 76.7%, comparable to other state-of-the-art grippers such as the commercial grippers 2F-140 and AG-105-145 models.

To compare the grasp types and the approximately straight motion of the fingertips of the proposed gripper with a conventional adaptive gripper, a performance comparison was conducted using the 2F-140 model, a commercial adaptive gripper with a stroke of 140mm, as shown in Fig. 13. This model is selected from Table 3 to verify the actual performance.

In Fig. 13 (a), the gripping motion of the commercial gripper is shown when grasping an object with a width of 36mm, and in Fig. 13 (b), it demonstrates grasping a cylinder

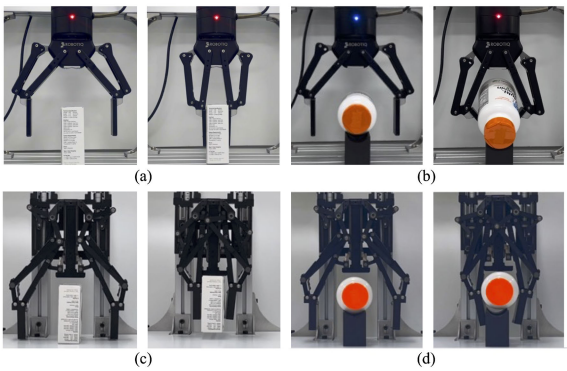


**FIGURE 13. Comparative grasping functions of commercial adaptive gripper and proposed gripper. Grasping motions of commercial adaptive gripper– (a) Grasping a box of 36mm width, (b) Grasping a cylinder of 65mm diameter. Grasping motions of proposed gripper– (c) Grasping the same object as in (a), (d) grasping the same object as in (b).**

of 65mm diameter using a power grasp. Fig. 13 (c) and (d) display the motions of the proposed gripper when grasping the same objects as the commercial gripper. In Fig. 13 (a), it is observed that the object is grasped through a curved trajectory of the fingertips, requiring adjustment to the appropriate height for gripping. In contrast, Fig. 13 (c) shows the proposed gripper grasping the object near the ground and achieving a palmar pinch grasp. During power grasp, it is noted that the commercial gripper cannot grasp an object of 65mm diameter, which aligns with the Introduction section stating that it can only grasp objects with a diameter of over 90mm. On the other hand, Fig. 13 (d) shows that the same-diameter object can be grasped through a palmar power grasp using the proposed gripper.

### D. VERIFICATION OF INCREASED GRASPING FORCE DURING PALMAR PINCH GRASP

It was theoretically confirmed in Fig. 10 that the increase in fingertip force is another characteristic of the power grip. To verify the actual increase in force and compare the theoretical and actual values, an experiment with a force/torque sensor (AFT-80, AIDIN ROBOTICS) was conducted as shown in Fig. 14. The experiment was conducted by gradually reducing the stroke by 20 mm from 140 mm, up to 50 mm considering the sensor size. As the proposed gripper is designed to automatically transition from a parallel or power grasp to a palmar pinch & power grasp, a screw was installed to selectively prevent the movement from transitioning to a palmar pinch grasp in order to measure the force before and after the power grasp. The input torque was 5 Nm at

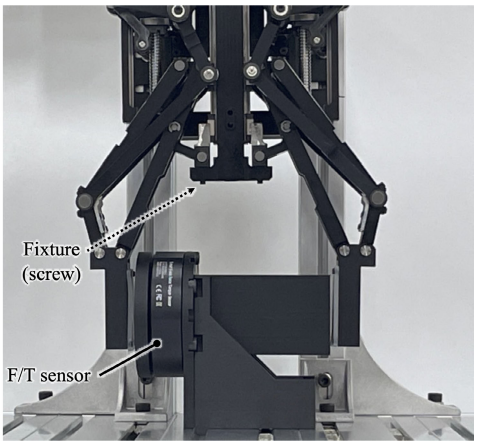


**FIGURE 14.** Experiment setup for the measurement of fingertip force.

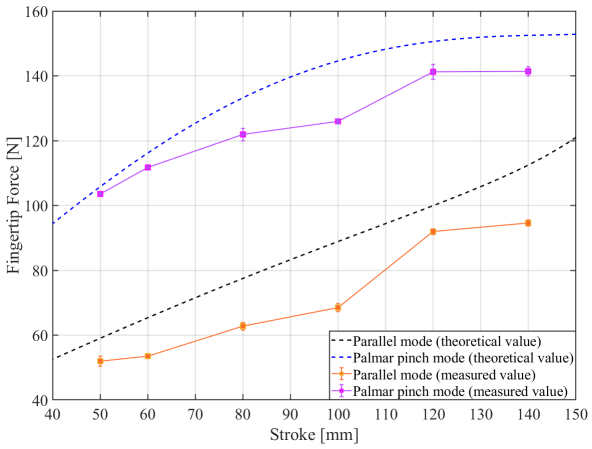


**FIGURE 15.** Comparison of theoretical values and sensor measurements between parallel mode and palmar pinch grasp mode.

joint A, and the calculated value was assumed to be the contact point of the fingertip on the second phalanx at a distance of 10mm from the contact point. Fig. 15 shows the graph of the measured force applied to the sensor and the theoretical value.

In Fig.15, it shows the calculated fingertip force values in parallel mode and palmar pinch mode for each stroke tested, as well as the standard deviation values measured by the sensor. Although there is a difference between the theoretically calculated value and the actual measured value, the trend is similar, and this difference can be attributed to friction in the mechanism, transmission efficiency, and differences in the contact position of the fingertip. As shown in the graph, it can be confirmed that the gripping force increases by an average of 57% during the stroke range as the fingertip moves in the palm direction before entering the palmar pinch grasp mode of the proposed gripper.

## VIII. CONCLUSION

In this paper, a new gripper with additional functionalities is proposed to address the limitations of existing adaptive grippers. By adding links to the gripper's structure, two key issues with existing adaptive grippers were addressed: the curved trajectory of fingertip movement and the decrease in the minimum size of graspable objects as the gripper stroke size increases. To ensure a straight-line trajectory for the gripper fingertips, the Grasshopper mechanism is employed, and to reduce the minimum size of objects that can be adaptively grasped, a palmar power grasp functionality was added. Additionally, the movement of the fingertips towards the palm is observed to increase the gripping force on the object, even with the same input torque. The functionality of the new gripper is verified by handling objects of various sizes and confirming that the minimum object size identified through theoretical calculations can indeed be grasped adaptively. This validation demonstrates that the proposed gripper is capable of adaptively grasping objects approximately 76.7% the size of an object's diameter relative to the gripper's stroke. A sensor is also utilized to compare the increase in contact force theoretically calculated when grasping objects with palmar power grasp mode versus the contact force generated in the parallel mode under the same torque input. Through this analysis, it was confirmed that there is a theoretical increase in grasping force of more than 57% on average.

Despite the successful implementation of the proposed features in the gripper, it still retains a limitation - objects smaller than the theoretically designed minimum size remain inaccessible during the process of palmar power grasping. For future work, it is planned that the efficiency of the proposed gripper in a picking system will be verified by integrating it with a manipulator, either alone or in combination with a suction gripper.

## APPENDIX A
## FORCE ANALYSIS

A more detailed explanation of (18) is as follows.

$$\begin{bmatrix} T_a & k\Delta\alpha \end{bmatrix} \begin{bmatrix} \dot{q}_a \\ \dot{\alpha} \end{bmatrix} = \begin{bmatrix} F_{cx} & F_{cy} \end{bmatrix} \mathbf{J_g} \begin{bmatrix} \dot{q_{5H}} \\ \dot{q}_t \end{bmatrix} \tag{21}$$

where the variable $k$ represents the torsion spring coefficient, while $J_g$ is the Jacobian matrix that represents the relationship between the velocity of the fingertip and the angle of each phalanx. If a virtual origin is established at joint $H$, $J_g$ can be represented as

$$\mathbf{J_g} = \begin{bmatrix} -l_5 \sin q_{5H} - k_2 \sin A & -k_2 \sin A \\ l_{5u} \cos q_{5H} + k_2 \cos A + l_{5d} \cot q_6 \sin q_{5H} & k_2 \cos A \end{bmatrix} \tag{22}$$

where A is $q_{5H} + q_t$. and $k_2$ is the contact location of the fingertip ($l_t$).

To determine the relationship between the actual input torque and the fingertip force, the relationship between the angular velocity term and the $\omega_i$ term on the right-hand side

can be used in the form of a Jacobian matrix, as shown below.

$$\begin{bmatrix} \dot{q_{5H}} \\ \dot{q_t} \end{bmatrix} = \mathbf{J_c} \begin{bmatrix} \dot{q_a} \\ \dot{\alpha} \end{bmatrix} \tag{23}$$

The $J_c$ in the proposed gripper link configuration can be obtained by following the steps below.

First, $q_{5H}$ and $q_6$ can be expressed as shown below through the geometrical relation.

$$l_6 \cos q_6 = l_{5d} \cos q_{5H} \tag{24}$$

Since $q_{5H}$ exists in (23), $q_6$ can be expressed as $q_{5H}$ through the above relationship. Subsequently, the relationship between the angular velocity of each joint can be determined by taking advantage of the closed-loop configuration of the five-link system composed of IJCDF. Here, $q_2$, $q_3$, $q_4$, and $q_{5H}$, $q_t$ have the following relationship.

$$\dot{q_2} + \dot{q_3} + \dot{q_4} = \dot{q_{5H}} + \dot{q_t} \tag{25}$$

By utilizing (25), it can be arranged into terms of $\dot{q_2}$ and $\dot{q_3}$, and $\dot{q_{5H}}$ and $\dot{q_t}$, as shown below.

$$\begin{bmatrix} -l_2 \sin q_2 - l_3 \sin \kappa & -l_3 \sin \kappa \\ l_2 \cos q_2 + l_3 \cos \kappa & l_3 \cos \kappa \end{bmatrix} \begin{bmatrix} \dot{q_2} \\ \dot{q_3} \end{bmatrix} = \begin{bmatrix} -l_4 \sin \upsilon + l_5 \sin (q_{5H}) & -l_4 \sin \upsilon \\ l_4 \cos \upsilon - l_5 \cos (q_{5H}) & l_4 \cos \upsilon \end{bmatrix} \begin{bmatrix} \dot{q_{5H}} \\ \dot{q_t} \end{bmatrix} \tag{26}$$

where the $\kappa$ is the $q_2 + q_3$ and $\upsilon$ is the $q_2 + q_3 + q_4$. In (26), the $2 \times 2$ matrix in the left term can be represented as $\mathbf{T_a}$ and the $2 \times 2$ matrix in the right term as $\mathbf{T_b}$, which are rewritten as

$$\begin{bmatrix} \dot{q_2} \\ \dot{q_3} \end{bmatrix} = \mathbf{T_a^{-1} T_b} \begin{bmatrix} \dot{q_{5H}} \\ \dot{q_t} \end{bmatrix} \tag{27}$$

This implies that the expression of $\dot{q_{5H}}$ and $\dot{q_t}$ in (23) can be represented by $\dot{q_2}$ and $\dot{q_3}$. Furthermore, the equation for $\dot{q_2}$ and $\dot{q_3}$ can be re-expressed as the relationship between $\dot{q_a}$ and $\dot{\alpha}$.

By utilizing the closed-loop relationship of $ABCJ$, the equation is a construct and the relationship is derived between $\dot{q_2}$ and $\dot{q_a}$ by taking the time derivative, as shown below.

$$\frac{\dot{q_2}}{\dot{q_a}} = \frac{-l_a \sin q_b}{l_2 \sin [q_2 - (q_a + q_b)] - E} \tag{28}$$

where $E$ is $[\sin (q_a + q_b)(l_{5d} \cot q_6 \sin q_{5H} - l_{5d} \cos q_{5H})]$.

The relationship between link 2 and link 3 also holds for $\dot{q_3}$, and since the sum of $q_3$ and $\alpha$ is always equal to $\pi$, the following relational expression can be obtained.

$$\dot{q_3} = -\dot{\alpha} \tag{29}$$

The equation is simplified as follows by summarizing the results.

$$\begin{bmatrix} \dot{q_{5H}} \\ \dot{q_t} \end{bmatrix} = \mathbf{T_a^{-1} T_b} \begin{bmatrix} X & 0 \\ 0 & -1 \end{bmatrix} \begin{bmatrix} \dot{q_a} \\ \dot{\alpha} \end{bmatrix} \tag{30}$$

where $X$ equals the right-hand term of (28).

In addition, it is necessary to derive the force applied when the fingers are moved towards the palm in power grasping mode after grasping an object. As shown in Fig. 6, the actual force required for this movement can be obtained using the Jacobian matrix to calculate the y-direction of the force at joint c caused by input torque.

The Jacobian matrix can be written as

$$\mathbf{J_p} = \begin{bmatrix} -l_a \sin q_a - l_b \sin q_a + q_b & -l_b \sin q_a + q_b \\ -l_a \cos q_a - l_b \cos q_a + q_b & l_b \cos q_a + q_b \end{bmatrix} \tag{31}$$

## REFERENCES

[1] J. Hernandez, M. S. H. Sunny, J. Sanjuan, I. Rulik, M. I. I. Zarif, S. I. Ahamed, H. U. Ahmed, and M. H. Rahman, "Current designs of robotic arm grippers: A comprehensive systematic review," *Robotics*, vol. 12, no. 1, p. 5, Jan. 2023.

[2] B. Zhang, Y. Xie, J. Zhou, K. Wang, and Z. Zhang, "State-of-the-art robotic grippers, grasping and control strategies, as well as their applications in agricultural robots: A review," *Comput. Electron. Agricult.*, vol. 177, Oct. 2020, Art. no. 105694.

[3] M. R. Cutkosky, "On grasp choice, grasp models, and the design of hands for manufacturing tasks," *IEEE Trans. Robot. Autom.*, vol. 5, no. 3, pp. 269–279, Jun. 1989.

[4] Robotiq. *2F-85 & 2F-140 Instruction Manual*. Accessed: Dec. 19, 2023. [Online]. Available: https://robotiq.com/products/2f85-140-adaptive-robot-gripper

[5] DH-ROBOTICS. *AG-160–95 & AG-105–145 Manual*. Accessed: Dec. 19, 2023. [Online]. Available: https://en.dh-robotics.com/product/ag

[6] T. Laliberté and C. M. Gosselin, "Underactuation in space robotic hands," in *Proc. 6th Int. Symp. Artif. Intell. Robot. Autom. Space (i-SAIRAS)*. Saint-Hubert, QC, Canada: Canadian Space Agency, Jun. 2001, pp. 1–8.

[7] L. A. Demers, S. Lefrançois, and J.-P. Jobin, "Gripper having a two degree of freedom underactuated mechanical finger for encompassing and pinch grasping," U.S. Patent S20 140 265 401 A1, Sep. 18, 2014.

[8] C. B. Teeple, T. N. Koutros, M. A. Graule, and R. J. Wood, "Multi-segment soft robotic fingers enable robust precision grasping," *Int. J. Robot. Res.*, vol. 39, no. 14, pp. 1647–1667, Dec. 2020.

[9] D. Yoon and K. Kim, "Fully passive robotic finger for human-inspired adaptive grasping in environmental constraints," *IEEE/ASME Trans. Mechatronics*, vol. 27, no. 5, pp. 3841–3852, Oct. 2022.

[10] M. Aqib, A. Imran, K. Khan, M. Arsalan, S. Manzoor, K. Long, and B. Yi, "Design and implementation of shape-adaptive and multifunctional robotic gripper," *J. Field Robot.*, vol. 41, no. 1, pp. 162–178, Jan. 2024.

[11] B. Kang and J. Cheong, "Development of two-way self-adaptive gripper using differential gear," *Actuators*, vol. 12, no. 1, p. 14, Dec. 2022.

[12] A. Kobayashi, J. Kinugawa, S. Arai, and K. Kosuge, "Design and development of compactly folding parallel open-close gripper with wide stroke," in *Proc. IEEE/RSJ Int. Conf. Intell. Robots Syst. (IROS)*, Nov. 2019, pp. 2408–2414.

[13] X. Li and W. Zhang, "Linearly parallel and self-adaptive robot hand with sliding base compensation for grasping on the surface," in *Proc. IEEE Int. Conf. Robot. Biomimetics (ROBIO)*, Dec. 2018, pp. 1822–1827.

[14] C. Luo and W. Zhang, "A novel straight-line mechanism and its application in robot design," in *Proc. 3rd Int. Conf. Adv. Robot. Mechatronics (ICARM)*, Jul. 2018, pp. 750–755.

[15] J. Li, Y. Kong, M. Dong, and R. Jiao, "Development of a linear-parallel and self-adaptive under-actuated hand compensated for the four-link and sliding base mechanism," *Robotica*, vol. 40, no. 6, pp. 2047–2064, Jun. 2022.

[16] Y. Liu and W. Zhang, "A robot gripper with differential and Hoecken linkages for straight parallel pinch and self-adaptive grasp," *Appl. Sci.*, vol. 13, no. 12, p. 7042, Jun. 2023.

[17] H. M. Passlov, A. Pontén, J. Björk, B. Rosén, M. Bruze, C. Svedman, and M. Isaksson, "Hand strength and dexterity in individuals with hand eczema," *J. Eur. Acad. Dermatology Venereology*, vol. 34, no. 12, pp. 2856–2862, Dec. 2020.

[18] A. Soleymani, A. Torabi, and M. Tavakoli, "A low-cost intrinsically safe mechanism for physical distancing between clinicians and patients," in *Proc. IEEE Int. Conf. Robot. Autom. (ICRA)*, May 2021, pp. 3677–3683.

[19] A. G. Ambekar, *Mechanism and Machine Theory*. New Delhi, India: PHI Learning, 2007.

[20] L. Birglen and C. M. Gosselin, "On the force capability of underactuated fingers," in *Proc. IEEE Int. Conf. Robot. Autom.*, Sep. 2003, pp. 1139–1144.
[21] L. Birglen and C. M. Gosselin, "Kinetostatic analysis of underactuated fingers," *IEEE Trans. Robot. Autom.*, vol. 20, no. 2, pp. 211–221, Apr. 2004.
[22] L. Birglen, T. Laliberté, and C. M. Gosselin, *Underactuated Robotic Hands*, vol. 40. Piscataway, NJ, USA: Springer, 2007.

**ISSAC RHEE** received the B.S. degree in mechanical engineering from Incheon National University, Incheon, South Korea, in 2017. He is currently pursuing the Ph.D. degree with the School of Mechanical Engineering, Sungkyunkwan University. He has been with the Robotics Innovatory Laboratory, School of Mechanical Engineering, Sungkyunkwan University, since 2017. His research interests include robotic mechanisms, human–robot interaction, and modeling and control.

**CHUN SOO KIM** received the B.S. and master's degrees in mechanical engineering from Sungkyunkwan University, Suwon, South Korea, in 2020 and 2022, respectively, where he is currently pursuing the Ph.D. degree in mechanical engineering. He has been with the Robotics Innovatory Laboratory, Sungkyunkwan University, since 2020. His research interests include human–robot interaction, dexterous robotic humanoid hands, grippers, and upper limb rehabilitation robots.

**HEEYEON JEONG** received the B.S. degree in mechanical engineering and the M.S. degree in AI robotics from Sungkyunkwan University, Suwon, South Korea, in 2019 and 2021, respectively, where he is currently pursuing the Ph.D. degree in mechanical engineering. He has been with the Robotics Innovatory Laboratory, Sungkyunkwan University, since 2021. His research interests include robotic gripper design and force/torque sensors.

**SEUNGHWAN UM** received the B.S. degree in mechanical engineering from Hanyang University (ERICA), Ansan, South Korea, in 2022. He is currently pursuing the Ph.D. degree with the School of Mechanical Engineering, Sungkyunkwan University. He has been with the Robotics Innovatory Laboratory, Sungkyunkwan University, since 2022. His research interests include mechanical design, grasping strategy, and manipulation.

**SEUNG JAE MOON** received the B.S. degree in mechanical engineering from Sungkyunkwan University, Suwon, South Korea, in 2019, where he is currently pursuing the Ph.D. degree in mechanical engineering. He has been with the Robotics Innovatory Laboratory, Sungkyunkwan University, since 2019. His research interests include force control, human–robot interaction, and real-time obstacle avoidance.

**YEONGGWANG SON** (Graduate Student Member, IEEE) received the B.S. degree in mechanical engineering from Halla University, Wonju, South Korea, in 2021. He is currently pursuing the Ph.D. degree with the School of Mechanical Engineering, Sungkyunkwan University. He has been with the Robotics Innovatory Laboratory, Sungkyunkwan University, since 2021. His research interests include computer vision and robotic grasping.

**YONG BUM KIM** received the B.S. degree in robotics from Ritsumeikan University, Kyoto, Japan, in 2012, and the Ph.D. degree in mechanical engineering from Sungkyunkwan University, Suwon, South Korea, in 2019. He is currently a Research Director with AIDIN ROBOTICS Inc., Anyang, South Korea. His research interests include force/torque sensors for robotics applications, control of a precision robot hand manipulator, surgical robots, and robot-sensing systems.

**HO SANG JUNG** received the B.S. and Ph.D. degrees in mechanical engineering from Sungkyunkwan University, Suwon, South Korea, in 2013 and 2021, respectively. He is currently with the Cobot Solution Team, AIDIN ROBOTICS Inc., Anyang, South Korea. His research interests include soft robotics, artificial muscles, tactile sensors, dexterous robotic hands, and manipulation.

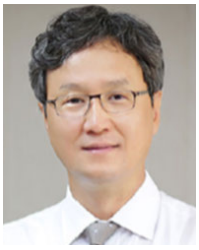

**HYOUK RYEOL CHOI** (Fellow, IEEE) received the B.S. degree in mechanical engineering from Seoul National University, Seoul, South Korea, in 1984, the M.S. degree in mechanical engineering from Korea Advanced Institute of Science and Technology (KAIST), Daejeon, South Korea, in 1986, and the Ph.D. degree in mechanical engineering from Pohang University of Science and Technology (POSTECH), Pohang, South Korea, in 1994.

From 1986 to 1989, he was an Associate Research Engineer with the IT Research Center, LG Electronics. From 1993 to 1995, he was a Postdoctoral Researcher with Kyoto University, Kyoto, Japan. From 1999 to 2000, he was a JSPS Fellow with the National Institute of Advanced Industrial Science and Technology (AIST), Japan. From 2008 to 2009, he was a Visiting Professor with Washington University, Washington, USA. Since 1995, he has been a Full Professor with the School of Mechanical Engineering, Sungkyunkwan University, Suwon, South Korea. His research interests include soft robotics, robotic mechanisms, field applications of robots, dexterous robotic hands, and manipulation.

Dr. Choi is the Co-Chair of the IEEE RAS Technical Committee, Robot Hand, Grasping and Manipulation. He was the General Chair of the 2012 IEEE Conference on Automation Science and Engineering (CASE), Seoul. He was an Editor of the *International Journal of Control, Automation and System*, a Technical Editor of IEEE/ASME TRANSACTIONS ON MECHATRONICS, and a Senior Editor of the *Journal of Intelligent Service Robotics*.